Ceramics International **23** (1996) 349–359
© 1997 Published by Elsevier Science Limited
Printed in Great Britain. All rights reserved
0272-8842/97 $17.00+0.00

PII: S0272-8842(96)00042-9

Preliminary Results on Preparation and Sintering Behaviour of Hafnia Powders

A. Lakhlifi,[a] M. Taha,[a,c] P. Satre,[a] Y. Jorand,[b] G. Fantozzi[b] & M. Roubin[a*]

[a]Université de Toulon et du Var. Matériaux à finalité spécifique (E.A. 1356). Laboratoire de Physicochimie du Matériau et du Milieu Marin, B.P. 132, 83957, La Garde Cedex, France
[b]INSA de Lyon. Groupe d'Etudes de Métallurgie Physique et de Physique des Matériaux (G.E.M.P.P.M) URA 341 CNRS 69621, Villeurbanne Cedex, France
[c]Université Hassan II, Faculté des sciences Ben M'sik, Casablanca, Morocco

(Received 12 December 1995; accepted 6 February 1996)

Abstract: In the present work, the characterization and sintering behaviour of hafnia prepared via thermolysis of an oxalic complex compound is investigated. The chemical formula of the complex is $H_2(HfO(C_2O_4)_2, 5H_2O)$. Yttria was added using an acid–base reaction in order to stabilize the hafnium oxide. The pyrolysis of the precursor was conducted using either a controlled calcination schedule or by introducing a chemical media which favours quick reaction. With the last route, the temperature rises very quickly.

Three batches of hafnia were prepared: pure, partially and fully stabilized. Morphology of the powders was investigated by means of SEM, porosimetric and specific surface area measurements. Then, green samples compacted up to 400 MPa were sintered or hot pressed in the range 1700–1900 °C. The density of sintered samples was largely dependent on the synthesis process and on the morphology of the green samples. © 1997 Published by Elsevier Science Limited

1 INTRODUCTION

When compared to zirconia, hafnia has received less study despite exhibiting the same phase transition (monoclinic, tetragonal and cubic). Researchers have been particulary interested in high temperature monoclinic–tetragonal phase transition of this oxide.

This toughening martensitic transformation occurs during heating at 1700 °C. From crystallographic point of view, hafnia, as zirconia, can be fully or partially stabilized using divalent or trivalent metallic oxides.[1]

Hafnia can be produced from $HfCl_4$, which can be extracted as an impurity during industrial processing of zirconia and thus merits attention.[2] Sinterable powders were prepared using softly like chemical method from the basic source of hafnia described above.

In the present article, some hafnia powders were prepared on a laboratory scale, characterized and sintered. Up to now hafnia powder has never been prepared using a flash reaction.

*To whom correspondence should be addressed.

2 EXPERIMENTAL PROCEDURE

Three batches of hafnia were prepared by thermolysis in solution of oxalic-hafnyl acid (Fig. 1). First, the solid $HfCl_4$ was dissolved in water and neutralized using ammonia. Hafnia hydroxid was obtained then filtered and washed before dissolution in an oxalic acid solution. Yttria was added using an acid–base reaction between the oxalic-hafnyl acid and yttria carbonate. The gel was obtained during water elimination and it was calcined below 500 °C to obtain hafnia.[3]

Another way to obtain hafnia is to promote flash pyrolysis by reacting an oxalic complex compound with $NH_4NO_3 + (CON_2H_3)_2$. The temperature of the reactor rises rapidly to a range of 1200–1300 °C and decreases very quickly to room temperature.[4]

Three batches of hafnia powder, referred to as A, B and C, corresponding to non-stabilized, fully

stabilized and partially stabilized hafnia, respectively, were prepared. The synthesis processes were as follows:

- Powder A was pure hafnia prepared using flash reaction;
- Powder B was 10 mol% yttria stabilized hafnia obtained using classic thermolysis of a precursor at 700 °C and a dwell time of 4 h at this temperature;
- Powder C is 3 mol% yttria stabilized hafnia prepared in a similar way to the powder B.

The powders were characterized by means of X-ray diffraction, SEM, sedimentation granulometry, mercury porosimetry and specific surface area. Compaction and sintering behaviour of these powders was studied extensively in order to compare the synthesis processes and the influence of composition at different yttria ratios.

Compaction tests were performed using mechanical testing apparatus. Samples of 2 g weight were compacted up to 200 MPa. The compaction rate was 0.5 mm/min.[5,6]

Mercury porosimetry was used in order to quantify pore size distribution. The measurements were conducted on samples compacted up to 400 MPa in an isostatic press.

Dilatometric behaviour was investigated using KCE high temperature vaccum dilatometer. The temperature schedule chosen was: a temperature increase first time to 1200 °C at a rate of 10 °C/min., then to 1700 °C at a rate of 5 °C/min., a dwell time of 2 h at this temperature and decrease to room temperature at a rate of 10 °C/min.

Some samples were compacted isostatically up to 400 °C and sintered using the same schedule as dilatometric investigations. Sintering was investigated in the range 1700–1900 °C.

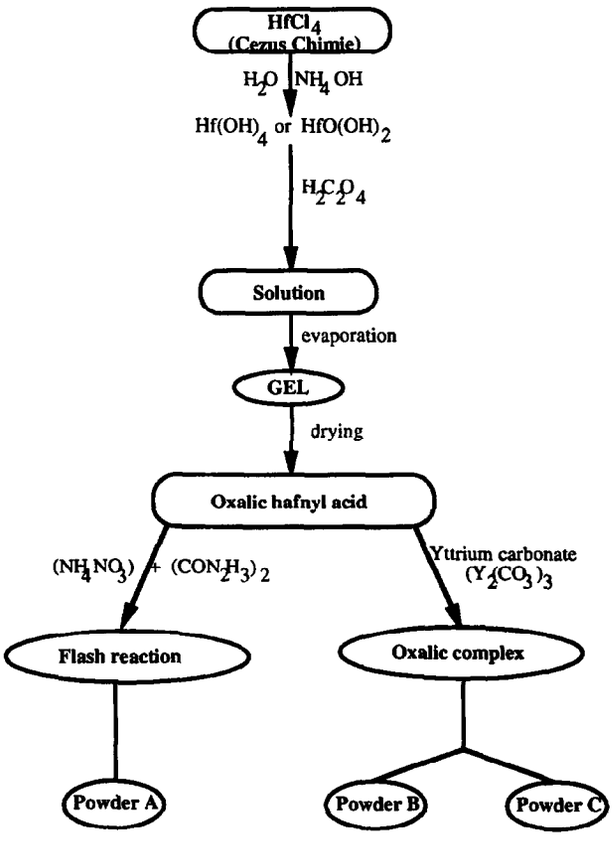

Fig. 1. Flowchart of the synthesis process of the powders.

3 RESULTS AND DISCUSSION

3.1 Powder characterization

Identification of the phase composition of specimens was carried out from XRD patterns (Fig. 2):

- powder A is 100% monoclonic;
- powder B is 100% cubic;
- powder C is formed from the tetragonal phase after elaboration at 700 °C, or composed of mixed monoclinic and tetragonal phases when calcined at higher temperatures.

Specific surface area was measured using the mercury method (Table 1). From these results it can be noted that powder B exhibits a lower surface area than powders A and C.

Figure 3 shows micrographs of the specimen morphologies. One can notice that agglomerates of powder A are small (50 μm) and more regular than those of the powders B and C (100 μm), which show clevage surfaces. Thus, powders B and C are largely hard aggregated.

3.2 Compaction behaviour

All batches show two compaction domains in the investigated range (Fig. 4). The domains correspond to agglomerate rearrangement and to the elimination of interagglomerate pores.[7,8] Some characteristics of the compaction behaviour of the powders are summarized in Table 2. We can note from these results, as shown in earlier work,[9] that powder A exhibits simultanously lower yield pressure and lower tap density than powders B and C. Thus, the agglomerates of powder A are less hard than the ones of powders B and C. Also, the agglomerates of powder A are smaller than the ones of powders B and C and their surface is rough, confering very low flow ability to this powder, causing low tap density. The large, densely packed B and C agglomerates lead to high tap density but their hardness is a disadvantage for interagglomerate

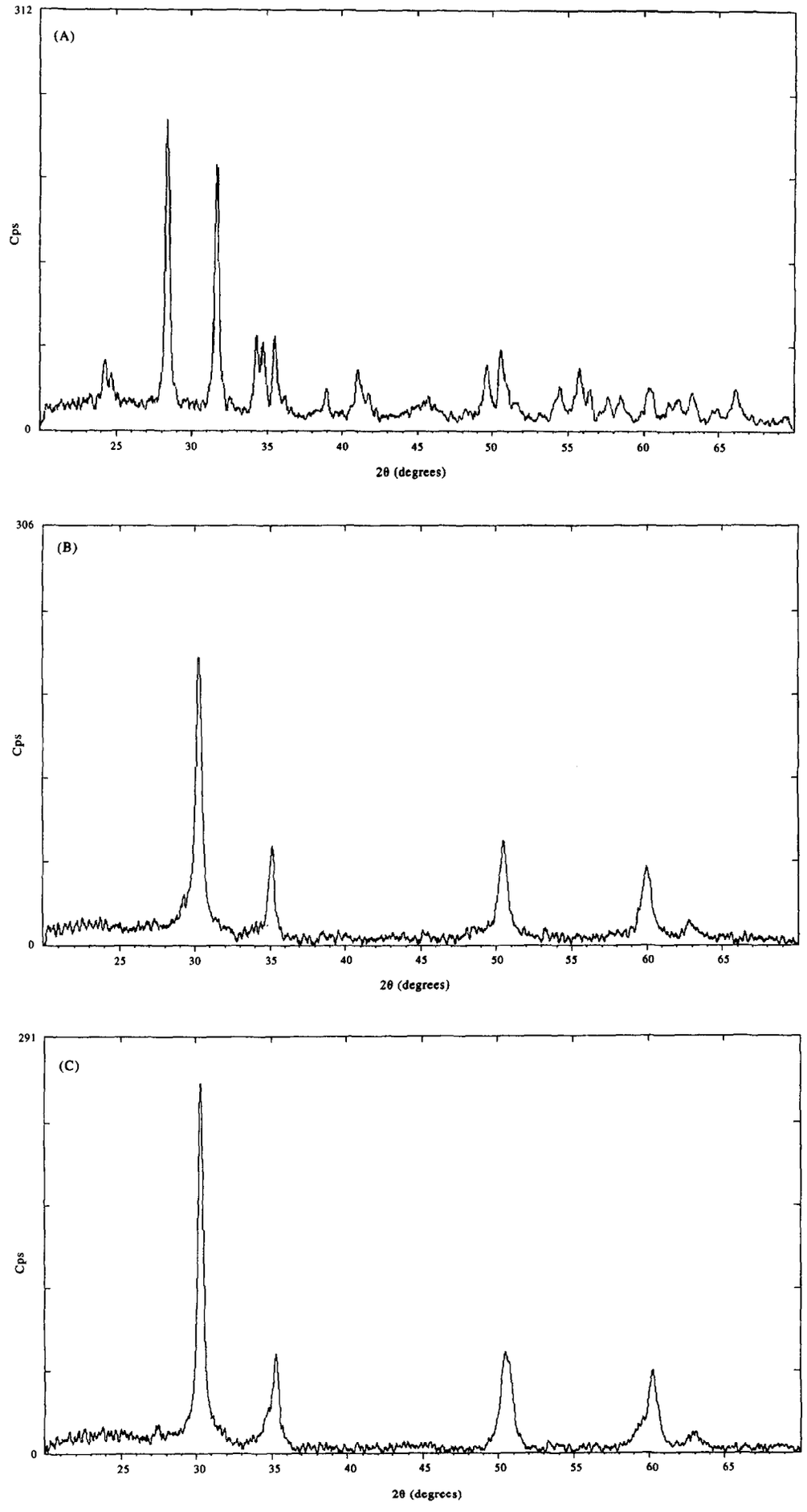

Fig. 2. X-ray patterns of the powders A, B and C.

Table 1. Characteristics of hafnia powders

	Synthesis route	Phase	Mol% Y_2O_3	S_w (m^2/g)	Agglomerate mean diameter (μm)	Crystallite mean diameter (TEM – nm)
A	Flash reaction	Monoclinic	0	5.1	50	20–50
B	Thermolysis	Cubic	10	2	100	10–30
C	Thermolysis	Tetragonal	3	10	>100	20–35

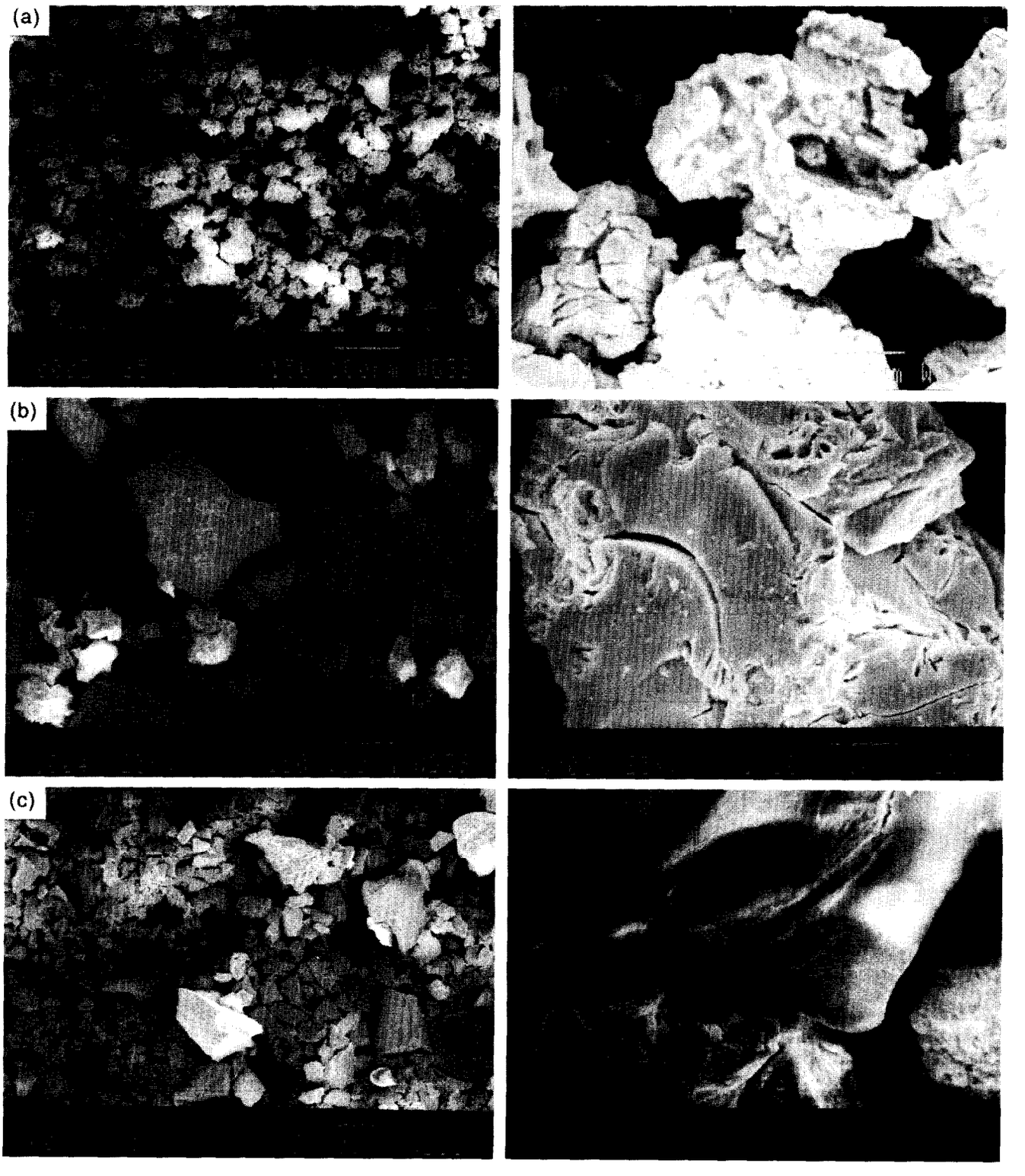

Fig. 3. SEM micrographs of starting powders.

pore elimination. Thus, the compacting efficiency p2 (Table 2) is lower for these powders (B and C).

(We note that p2 is the slope of high pressures linear region.)[10]

3.3 Characterization of green samples

From the results in Table 2 and Fig. 5 it can be noted that compacted powder A exhibits a monomodal pore distribution localized in the range 0.006–0.1 μm. Compacted B and C samples exhibit bimodal pore distributions, even when compacted up to 400 MPa. Thus, in agreement with the SEM observations, these powders are more aggregated than powder A.

3.4 Dilatometric analysis

Figure 6 illustrates the shrinkage behaviour of samples A, B and C isostatically compacted up to 400 MPa before sintering. Densification of samples A, B and C begins, respectively, at 1200, 1100 and 1000 °C. At this sintering stage, elimination of intercrystallite porosity begins. Samples B and C having very small intercrystalline porosity, as shown by means of porosimetry investigations, began to sinter at lower temperatures than sample A, but their shrinkage is delayed until the high temperature region. This is caused by the aggregation of these powders. On the contrary, sample A shrinks in one step evolution and major porosity was eliminated. So, high shrinkage was obtained for this sample.

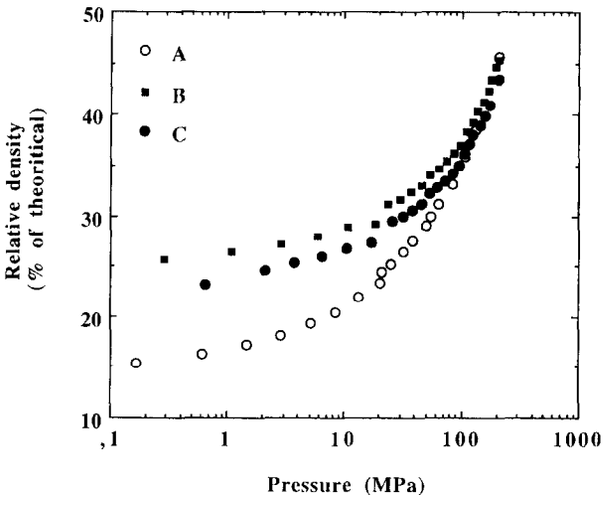

Fig. 4. Compaction curves of the powders pressed up to 200 MPa.

3.5 Sintering behaviour

Values of density for sintered samples versus sintering temperature are gathered in Table 3. For samples B and C, density increases with increasing sintering temperature but does not reach theoretical value (respectively, 10.3 and 9.7 for cubic and monoclinic phases). As shown in dilatometric observations, sintering is inhibited by the presence of large porosity which is caused by a large aggregation of starting powder. For powder A, a density of 95% of the theoretical value was reached at 1700 °C. The sintering domain of this unstabilized powder remains limited by monoclinic–tetragonal phase transition, whenever an attempt was made to increase sintering temperature for increasing density. So, density of this sample decreases with increasing temperature owing to microcracking caused by phase transformation during cooling.

The three powders were 4 MPa hot pressed in order to increase sintering efficiency. The temperature schedule was similar to the one used in the dilatometry measurements. Powder A samples either hot pressed at 1800 °C for 2 h or at 1500 °C for 2 h, failed because of phase transition causing microcracking as confirmed by porosimetry (Fig. 7). The density of 1900 °C hot pressed sample B, containing cubic phase, reaches theoretical value. Also, for sample C, which is hot pressed at 1800 °C, the density is 95% of theoretical.

All samples either sintered in vaccum furnace or hot pressed in a graphite die are black coloured. We have noted that the colour can't be by-passed in the two cases.

3.6 X-ray characterization of sintered samples

X-ray diffraction was carried out on the samples in order to clarify the origin of the black coloration.

Table 2. Compaction characterstics and pore size distribution of samples A, B and C

	Compaction characterstics				Pore size distribution of samples compacted up to 400 MPa (μm)	
	Density (% dth)		Slope	*P*j	Intercrystallites	Interagglomerates
	Tap density	200 MPa	p2	(MPa)		
A	15.6	45.6	32.0	30	0.006–0.1	—
B	25.6	45.2	25.6	55	0.003–0.05	1–3
C	23.1	43.4	23.9	50	0.003–0.009	0.3–4

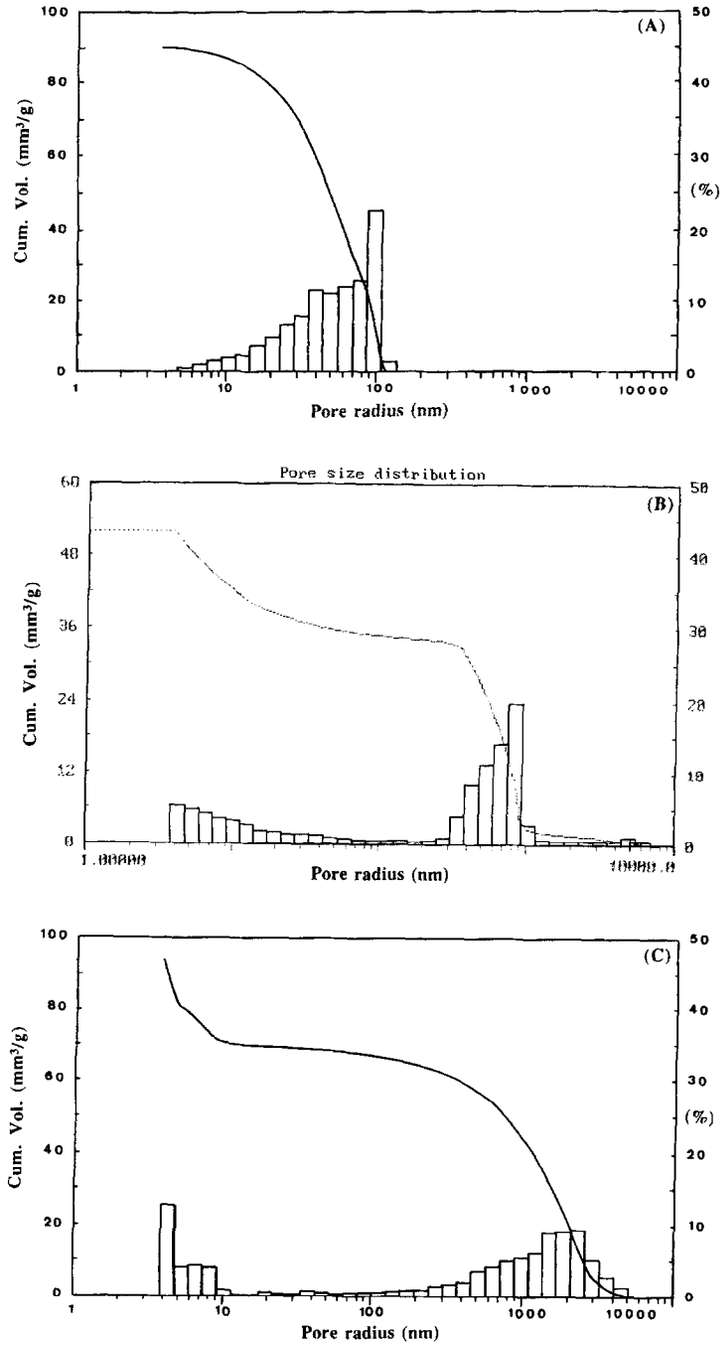

Fig. 5. Pore size distribution of green samples compacted isostatically up to 400 MPa.

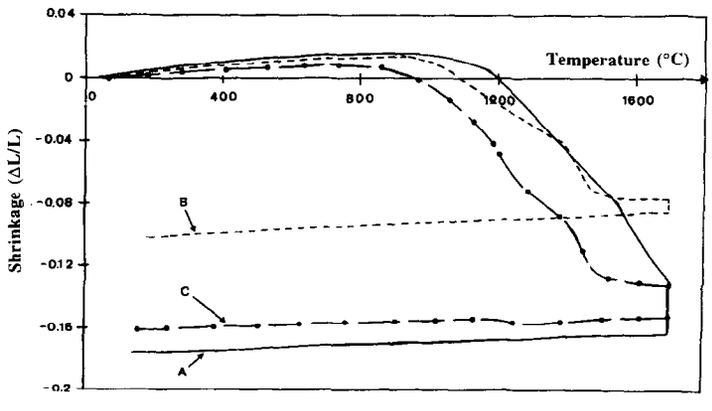

Fig. 6. Dilatometric curves of samples A, B and C compacted isostatically up to 400 MPa.

We have noted that the presence of hafnium carbide is responsible for the phenomenon whenever samples A, B or C are sintered at a temperature higher than 1750 °C (Fig. 8). The formation of hafnium carbide is due to the presence of carbon in the furnace. The thickness of the HfC layer is dependent on factors such as density of the sample or the sintering temperature controlling formation.

Table 3. Sintering density data

	Density of sintered samples (g/cm^3)				
	1700 (2h)	1700 (4h)	1750 (2h)	1800 (2h)	1900 (2h)
A	8.67	9.23	9.01	8.49	—
B	6.22	5.91	—	6.2	6.38
C	6.94	6.53	—	6.71	6.94

Also, we have noted that the scattering peaks of sample B are slightly displaced when compared to JCPDS for cubic hafnia. The deviation for the higher 2Θ angle is more significant than the one for lower values of 2Θ angles. This phenomena can be explained by distortion of a network (Fig. 9).

3.7 Thermal analysis

The analysis described above was not adequate to explain the presence of the black colour in samples sintered at 1700 °C in which no hafnia carbide was detected. So, we thought, as described in earlier zirconia work,[11] the phenomena may be the result of non-stoichiometry of HfO_2. So, TGA was carried out on sintered samples in an oxygen atmo-

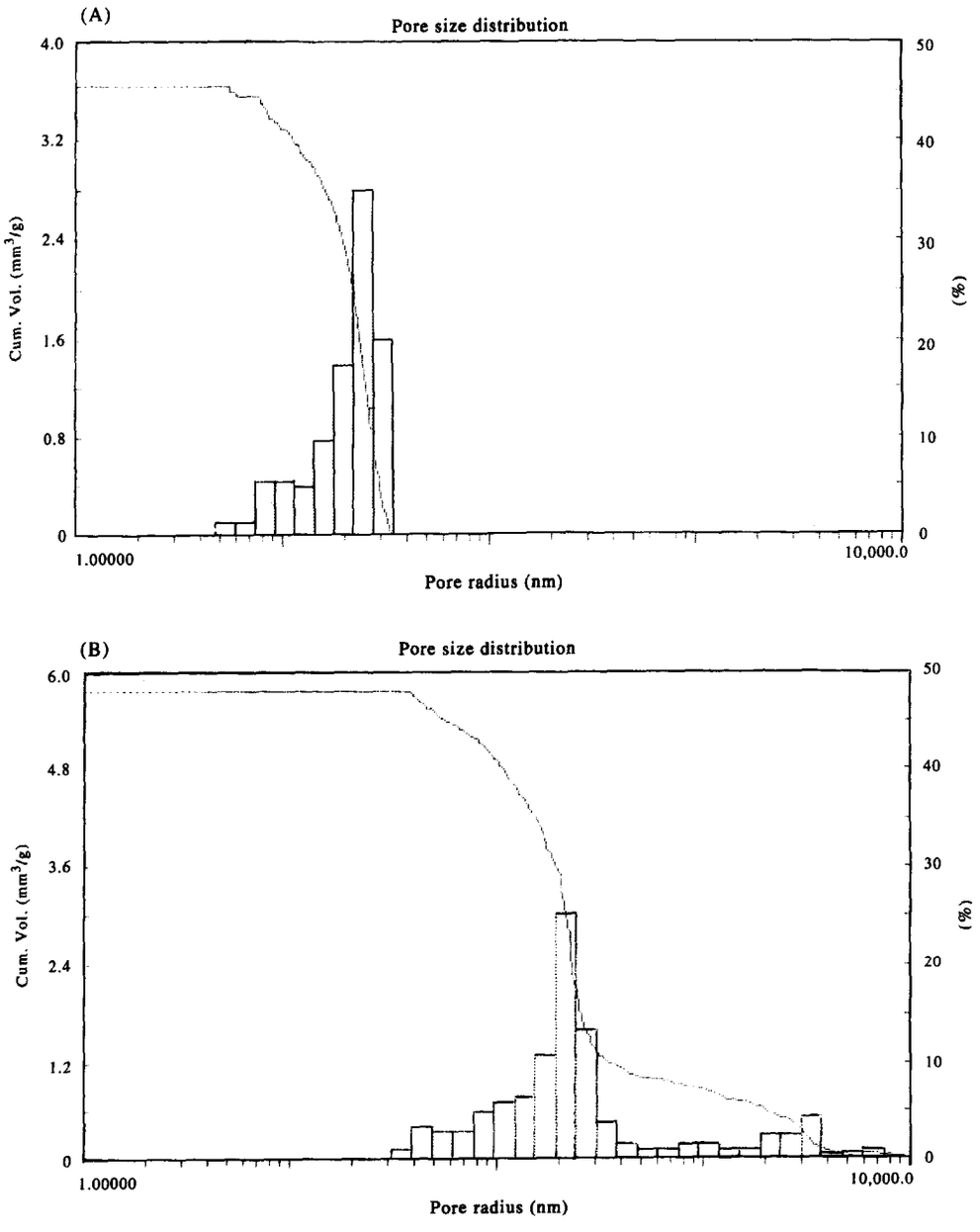

Fig. 7. Pore size distribution of sample A: (a) sintered at 1700 °C; (b) hot pressed at 1800 °C.

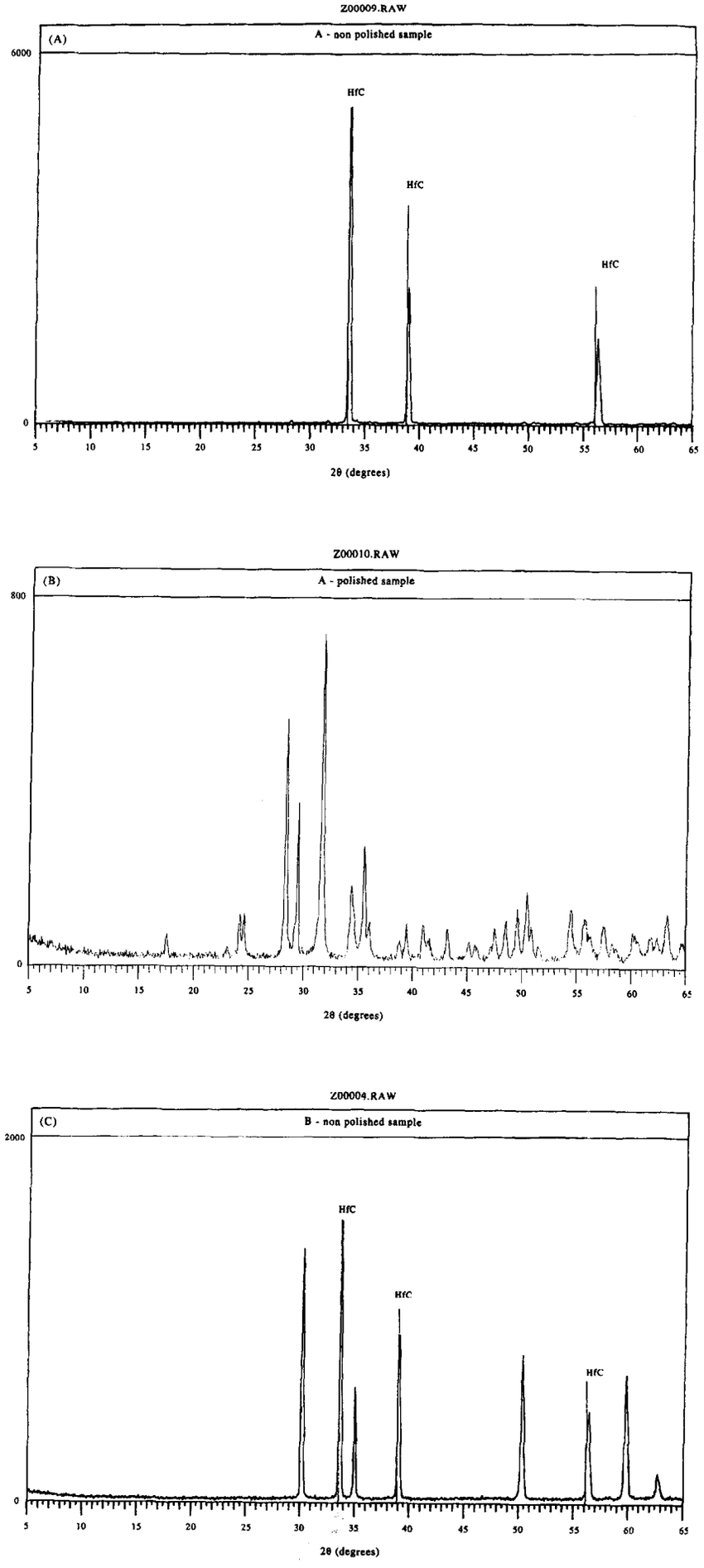

Fig. 8. X-ray patterns of sintered samples exhibiting HfC formation: sample A at 1750 °C; samples B and C at 1900 °C.

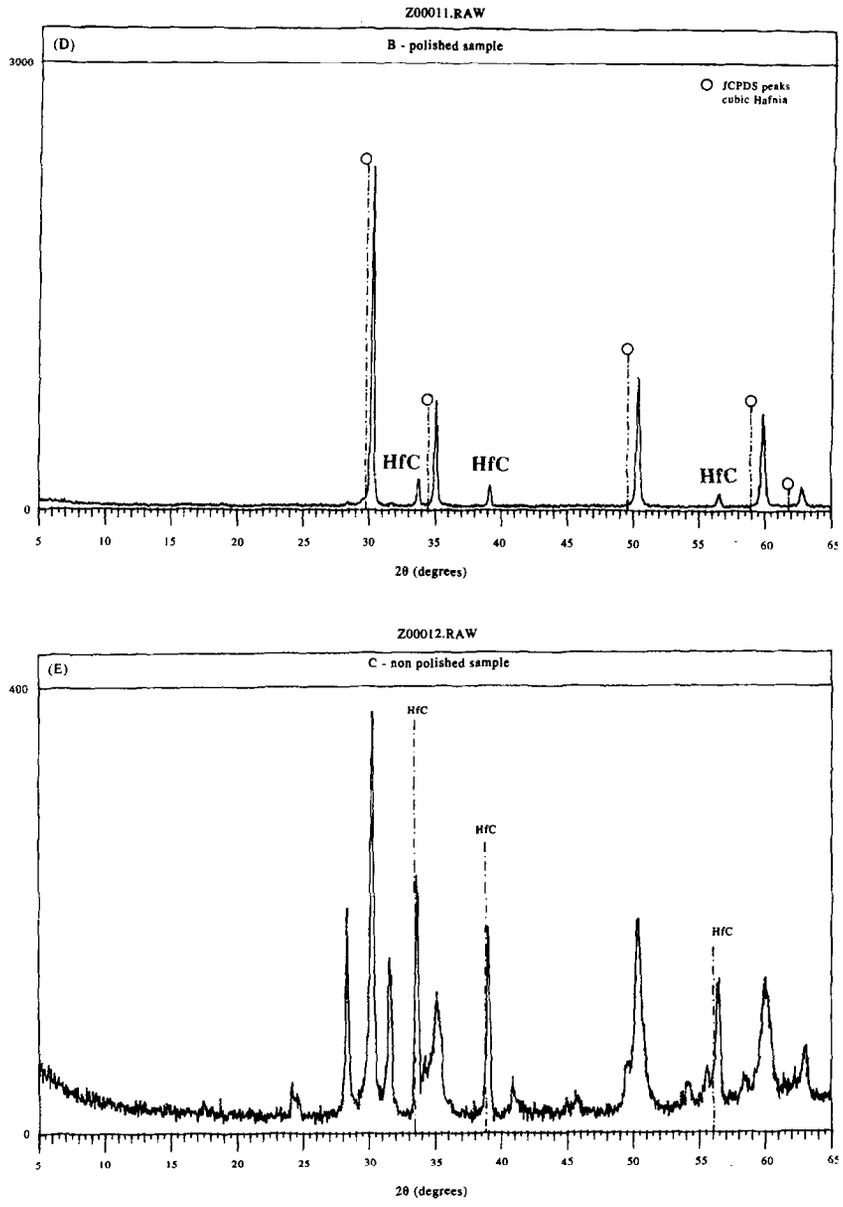

Fig. 8. *cont.*

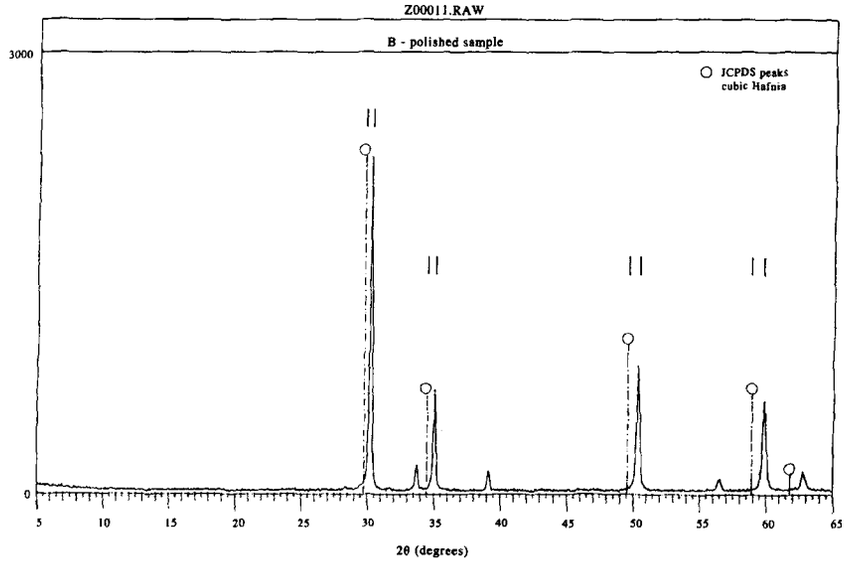

Fig. 9. X-ray patterns of sample B sintered at 1900 °C and polished, exhibiting distortion of network [idem Fig. 8(D)].

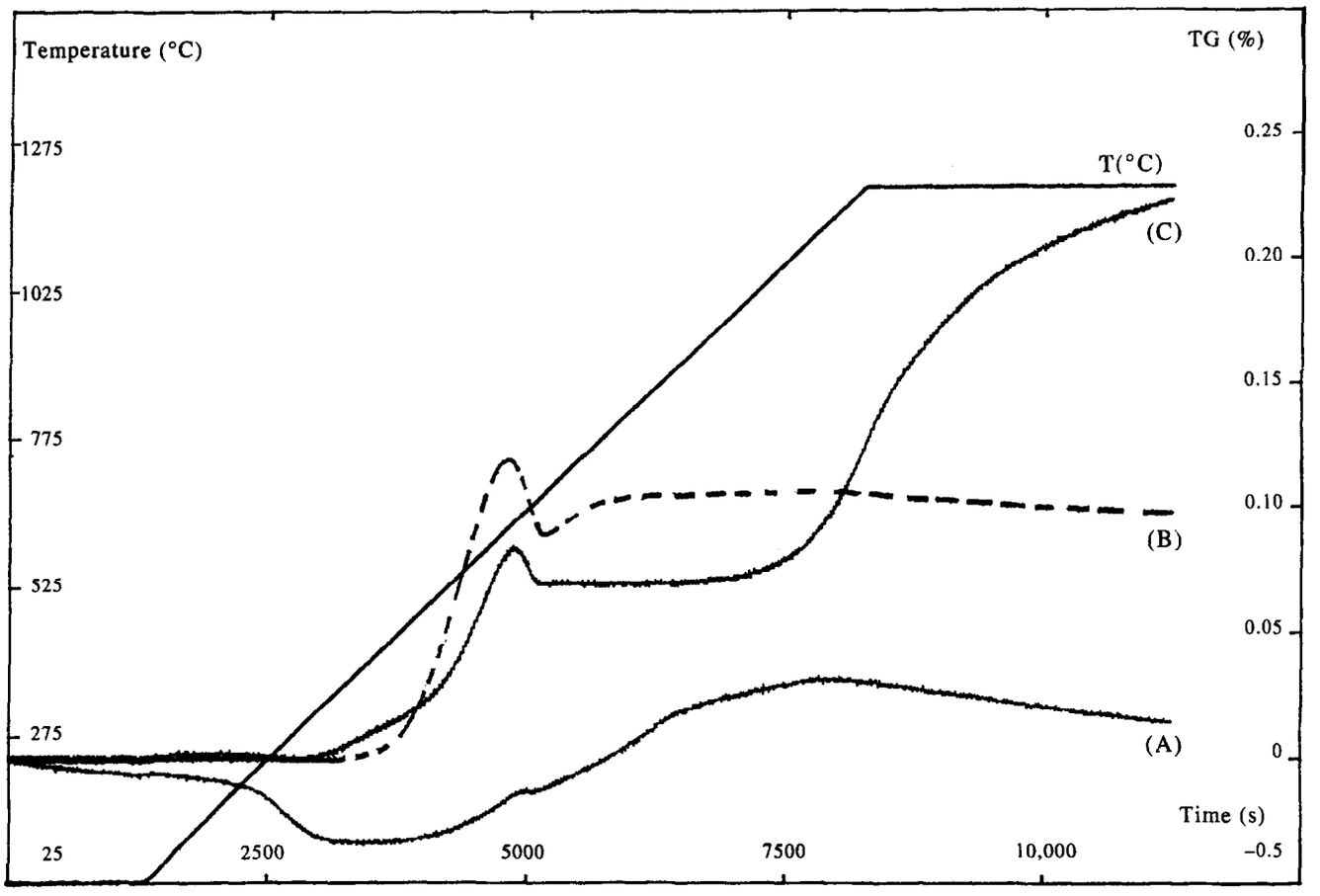

Fig. 10. DTA curves (600 °C/h) of 1700 °C vacuum sintered samples.

sphere. Figure 10 shows thermal effects versus calcination temperature. The behaviour of these samples is quite different: for B and C, as the weight increases, then passes through a maximum value at 630 °C. This is probably caused by an adsorption of oxygen which reacts with HfC according to the following reaction: $HfC + 2\,O_2 \rightarrow HfO_2 + CO_2$. The DTA measurement shows an exothermic effect corresponding to this reaction at the same level of temperature. Then, slight weight loss, corresponding to CO_2 desorption, is seen. The weight variation below 700 °C is more important for the biphasic sample C than for the one phase samples: A (monoclinic) or B (cubic). Also, the weight of sample B increases when the temperature was kept constant at a value higher than 700 °C, this phenomena can be explained by the presence of a large heterogeneity in the sintered sample. In fact, the presence of imperfections at grain boundaries favours formation of non-stoichiometric HfO_2.

4 CONCLUSION

This work gives some preliminary results concerning sintering behaviour of pure, partially and fully stabilized hafnia prepared using thermolysis of an oxalic complex. Also, three different powders prepared in different ways were characterized. Therefore, the following conclusions may be drawn:

1. The processing route greatly influences the morphology of the powder depending on the manner in which the thermolysis of precursor was conducted.
2. Powder A prepared using a flash reaction sinters well when compared to the other powders, but the density of the sintered sample does not reach the theoretical value even when hot pressed. Sintering in the monoclinic domain was limited by the monoclinic–tetragonal transition causing microcracks.
3. Powders B and C, prepared using classic thermolysis, exhibit bimodal pore distributions owing to the presence of aggregates. Thus, for densification up to 95% of theoretical, hot pressing is necessary.
4. Formation of hafnium carbide at the surface or in volume of samples is unavoidable when samples are sintered over 1750 °C in a carbon furnace or in a hot pressed graphite die.
5. Thermal analysis under oxygen flux shows that carbon departure can also be correlated to the presence of non-stoichiometric hafnia when the samples are sintered at 1700 °C in a vacuum furnace.

ACKNOWLEDGEMENTS

It is a pleasure to acknowledge help from Dr M. Jebrouni, Professor B. Durand and Dr J. P. Deloume with porosimetric measurements and stimulating discussions.

REFERENCES

1. WANG, J., LI, H. P. & STEVENS, R., Review: Hafnia and hafnia toughened ceramics. *J. Mater. Sci.*, **27** (1992) 5397–5430.
2. LAKHLIFI, A., Elaboration de poudres d'oxyde d'hafnium à partir de précurseurs oxalique et leur caractérisation. PhD Thesis: UTV (Toulon), France, 1995.
3. LAKHLIFI, A., SATRE, P., SEBAOUN, A. & ROUBIN, M., *Ann. Chim. Fr.*, **18** (1993) 565.
4. LAKHLIFI, A., LEROUX, CH., SATRE, P., ROUBIN, M. & NIHOUL, G., Hafnia powders (HfO_2): elaboration and characterization by TEM. *J. Sol. State Chem.*, **119** (1995) 289–298.
5. JORAND, Y., TAHA, M., MISSIAEN, J. M. & MONTANARO, L., Compaction and sintering behaviour of sol–gel powders. *J. Eur. Ceram. Soc.*, **15** (1995) 469–477.
6. TAHA, M., PALETTO, J., JORAND, Y., FANTOZZI, G., SAMDI, A., JEBROUNI, M. & DURAND, B., Compaction and sintering behaviour of zirconia powders. *J. Eur. Ceram. Soc.*, **15** (1995) 759–768.
7. HOLMAN, L. E., The compaction behaviour of particulate materials: an elucidation based on percolation theory. *Powder Technol.*, **66** (1991) 265–280.
8. MESSING, G. L., MARKHOFF, C. J. & McCOY, L. G., Characterization of ceramic powder compaction. *Ceram. Bull.*, **61**(8) (1982) 857–860.
9. DYNYS, F. W. & HALLORAN, J. W., Influence of aggregates on sintering. *J. Am. Ceram. Soc.*, **67**(9) (1984) 596–601.
10. ZHENG, J. & REED, J. S., Particle and granule parameters affecting compaction efficiency in dry pressing. *J. Am. Ceram. Soc.*, **71**(11) (1988) C456–C458.
11. JORAND, Y., Elaboration et caractérisation de composites dispersoïdes ternaires base Alumine–Zircone à vocation thermomécanique. PhD Thesis: INSA de Lyon, France, 1991.